The Journal of Infectious Diseases

MAJOR ARTICLE

Shear-Resistant Binding to von Willebrand Factor Allows *Staphylococcus lugdunensis* to Adhere to the Cardiac Valves and Initiate Endocarditis

Laurens Liesenborghs,[1] Marijke Peetermans,[1] Jorien Claes,[1] Tiago Rafael Veloso,[1] Christophe Vandenbriele,[1] Maarten Criel,[1] Marleen Lox,[1] Willy E. Peetermans,[2] Simon Heilbronner,[3] Philip G. de Groot,[4] Thomas Vanassche,[1] Marc F. Hoylaerts,[1] and Peter Verhamme[1]

[1]Center for Molecular and Vascular Biology, and [2]Department of Internal Medicine, KU Leuven, Belgium; [3]Interfaculty Institute of Microbiology and Infection Medicine, University of Tübingen, Germany; and [4]Laboratory of Clinical Chemistry and Haematology, University Medical Center, Utrecht, The Netherlands

Background. *Staphylococcus lugdunensis* is an emerging cause of endocarditis. To cause endovascular infections, *S. lugdunensis* requires mechanisms to overcome shear stress. We investigated whether platelets and von Willebrand factor (VWF) mediate bacterial adhesion to the vessel wall and the cardiac valves under flow.

Methods. *S. lugdunensis* binding to VWF, collagen, and endothelial cells was studied in a parallel flow chamber in the absence and presence of platelets. In vivo adhesion of *S. lugdunensis* was evaluated in a mouse microvasculature perfusion model and a new mouse model of endocarditis.

Results. Contrary to other coagulase-negative staphylococci, *S. lugdunensis* bound to VWF under flow, thus enabling its adhesion to endothelial cells and to the subendothelial matrix. In inflamed vessels of the mesenteric circulation, VWF recruited *S. lugdunensis* to the vessel wall. In a novel endocarditis mouse model, local inflammation and the resulting release of VWF enabled *S. lugdunensis* to bind and colonize the heart valves.

Conclusions. *S. lugdunensis* binds directly to VWF, which proved to be vital for withstanding shear forces and for its adhesion to the vessel wall and cardiac valves. This mechanism explains why *S. lugdunensis* causes more-aggressive infections, including endocarditis, compared with other coagulase-negative staphylococci.

Keywords. *Staphylococcus lugdunensis*; shear stress; platelets; von Willebrand factor; endocarditis; endothelial cells.

Staphylococcus lugdunensis is an emerging species of coagulase-negative staphylococci. Although *S. lugdunensis* is part of the normal skin flora, it has an increased virulence as compared to other coagulase-negative staphylococci [1]. Since its discovery, a mere 25 years ago, *S. lugdunensis* has gained notoriety for causing a destructive form of infective endocarditis, with a mortality rate of up to 40% [2]. However, little is known about the virulence factors of this insidious pathogen.

To cause endovascular infections bacteria require a mechanism to overcome the shear stress of flowing blood. Shear stress, defined as physical stress caused by the displacement of blood relative to the vessel wall, creates a frictional force that bacteria need to endure if they want to adhere to the vasculature [3]. This is especially the case in infective endocarditis, since the heart valves are exposed to considerable shear forces [4].

Following vascular injury, platelets overcome shear stress by binding to von Willebrand factor (VWF). VWF is a large multimeric protein that is secreted from and temporarily retained on activated endothelial cells. In addition, circulating VWF multimers can accumulate in the subendothelial matrix if the vascular integrity is breached. When bound VWF is exposed to the blood flow, the resulting shear forces unfold the molecule and expose previously concealed domains to which platelets can bind [5].

Most pathogens that cause endocarditis bind and activate platelets and use platelets as a bridge to overcome shear stress [6, 7]. Moreover, besides activating platelets, *Staphylococcus aureus* also interacts directly with VWF in a shear-dependent manner via its VWF-binding protein [8, 9]. Also for *S. lugdunensis* a cell wall-anchored protein with the potential to bind VWF has been reported [10]. However, the exact function of this VWF-binding protein of *S. lugdunensis* (vWbl) remains unclear.

In this study, we explored whether platelets and VWF promote the adhesion of *S. lugdunensis* under flow and play a role in *S. lugdunensis* endocarditis.

MATERIALS AND METHODS

Bacterial Strains

S. lugdunensis N920143, derived from a breast abscess in 1992, and *S. aureus* Newman were used. Clinical strains of *S. lugdunensis,*

Received 20 July 2015; accepted 19 December 2015; published online 6 January 2016.

Presented in part: XXVth Congress of the International Society on Thrombosis and Haemostasis, Toronto, Canada, 20–25 June 2015. Abstract AS009.

Correspondence: L. Liesenborghs, Center for Molecular and Vascular Biology, KU Leuven, Leuven, Belgium, Box 480, Herestraat 49, 3000 Leuven, Belgium (laurens.liesenborghs@med.kuleuven.be).

The Journal of Infectious Diseases® 2016;213:1148–56

DOI: 10.1093/infdis/jiv773

Staphylococcus epidermidis, Staphylococcus capitis, Staphylococcus haemolyticus and *Staphylococcus hominis* were isolated from blood cultures of patients from the University Hospitals of Leuven. Bacteria were grown in tryptic soy broth overnight. Mutants deficient in the vWbl, fibrinogen-binding protein (Fbl), and sortase A (SrtA) genes were created by electroporation with plasmid DNA as previously described [11].

Platelet Aggregation

Platelet-rich plasma was obtained as previously described [7]. Collagen I (1 mg/mL; Takeda, Linz, Austria), *S. aureus* (OD_{600} 2.0; 1×10^8 colony-forming units [CFU]/mL), or *S. lugdunensis* (OD_{600} 2.0; 1×10^8 CFU/mL) were added, and aggregation was measured by light transmission aggregometry in a Chrono-Log aggregometer (Kordia, Leiden, the Netherlands).

Perfusion Experiments

Bacteria were labeled with 5(6)-carboxy-fluorescein N-hydroxysuccinimidyl ester (Sigma-Aldrich, Darmstadt, Germany; 30 µg/mL) for 30 minutes, quantified through optical densitometry, and diluted to a concentration of 15×10^7 CFU/mL in phosphate-buffered saline [PBS], human plasma, VWF-deficient plasma (Nodia, Boom, Belgium), or PRP, as indicated. When specified, soluble VWF (Haemate, CSL Behring, Mechelen, Belgium) or VWF deletion mutants [12] were added.

We used a micro-parallel flow chamber (in-house design), in which coverslips coated with VWF (50 µg/mL) or collagen I (160 µg/mL) or seeded with human blood outgrown endothelial cells (BOECs) were mounted. BOECs were isolated as previously described [13] and grown in EGM-2 medium (Lonza, Basel, Switzerland). Cells were activated by perfusion with 0.1 mM of the Ca^{2+}-ionophore A23187 (Sigma-Aldrich, Germany) for 5 minutes.

Fluorescent-labeled bacteria were perfused with a high-accuracy pump (PHD 2000 Infusion; Harvard Apparatus, Holliston, Massachusetts) for 10 minutes. Shear rate, defined as the velocity gradient measured across the diameter of the flow chamber [$\gamma = 6Q/wh^2$] and denoted in inverse seconds, was adjusted through the flow rate. Pictures were taken with an inverted microscope (Axio-observer DI; Carl-Zeiss, Zaventem, Belgium) at 20-fold magnification. Fluorescence was quantified with ImageJ (National Institutes of Health, Bethesda, Maryland) and denoted as arbitrary fluorescent units.

For immunofluorescence staining, samples were fixed with paraformaldehyde 4% under flow. A polyclonal anti-VWF rabbit antibody (31 µg/mL; Dako, Glostrup, Denmark) served as primary antibody, and a goat anti-rabbit Alexa Fluor-568 (20 µg/mL; Invitrogen, Grand Island, New York) served as secondary antibody. Images were obtained on a Zeiss ELYRA Superresolution Microscope (Carl-Zeiss, Belgium).

Mesenteric Perfusion Model

The institutional ethics committee approved all animal experiments (license number 110/2014). In the mesenteric perfusion model [8] C57Bl/6 wild-type (WT) mice or VWF homozygous knockout (*Vwf* $^{-/-}$) mice were used. We anesthetized the mice, using ketamine and xylazine, and catheterized the right jugular vein (Portex intravenous cannula, 2F, OD). The abdominal cavity was opened, and the mesenteric microcirculation was visualized with an inverted microscope (Axio-observer D1). By local application of 5 µL of the Ca^{2+}-ionophore A23187 (10 mM) the vascular endothelium was activated, and 100 µL of carboxy fluorescein–labeled bacteria (5×10^8 CFU/mL) was injected. Live images were obtained via video-based microscopy at 20-fold magnification. The fluorescent signal in the vessels was quantified manually with ImageJ and reported as arbitrary fluorescent units.

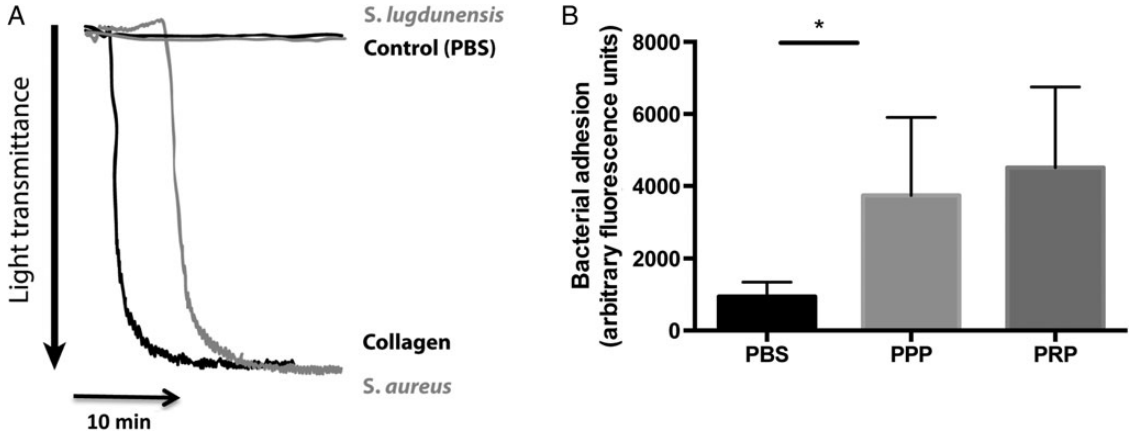

Figure 1. *Staphylococcus lugdunensis* does not activate platelets. *A*, Platelet aggregation measured by light transmission aggregometry of platelet-rich plasma (PRP) after addition of phosphate-buffered saline (PBS), collagen (1 µg/mL), *Staphylococcus aureus* Newman (10^8 colony-forming units [CFU]/mL), or *S. lugdunensis* N920143 (10^8 CFU/mL). *B*, Adhesion of *S. lugdunensis* N920143 to collagen-coated coverslips in a micro-parallel flow chamber, in the presence of buffer, platelet-poor plasma (PPP), or PRP. Results are expressed as mean ± SD (n = 6). **P* < .05, by the 2-tailed paired Student *t* test.

Standard Mouse Endocarditis Model

The standard mouse model of endocarditis is described elsewhere [14]. The right carotid artery of WT and *Vwf*$^{-/-}$ C57Bl/6 mice was exposed and ligated below the bifurcation. A small wire (Ethylon 4.0; Ethicon, Cornelia, Georgia) was inserted and moved upstream beyond the aortic valve until pulsation of the thread was detected. After fixating the wire, we closed the skin. *S. lugdunensis* (3×10^6 CFU) was injected intravenously 24 hours after surgery. Mice were monitored for survival 4 times per day up to day 7.

For histologic analysis, the mice were perfused with saline and paraformaldehyde both for 3 minutes, and the hearts were embedded in paraffin and stained with Brown–Hopps tissue Gram stain.

Inflammatory Mouse Endocarditis Model

For this model the same mouse strains were used. We exposed the carotid artery and inserted a 32-gauge polyurethane catheter (RecathCo, Allison Park, Pennsylvania). The catheter was moved upstream until pulsation of the catheter was detected and was connected to a high-accuracy pneumatic pump that generated an infusion rate of 10 µL/min. The mice received an infusion of saline or 200 mM histamine (Sigma-Aldrich, Darmstadt, Germany) in saline for 5 minutes, followed by 10-minute perfusion with *S. lugdunensis* (3×10^6 CFU/mL). Afterwards, the mice were euthanized, and histologic analysis of the hearts was performed as described above. Sections of the aortic valve were analyzed with the ImageJ analysis software, and mean vegetation size was measured. To analyze bacterial adhesion, fluorescent-labeled bacteria were infused, and cryosections of the aortic valves were analyzed for fluorescence with ImageJ. In another set of experiments, the catheter was removed, and the mice were allowed to recover. Surviving mice were euthanized after 3 days, and the hearts were harvested for histologic analysis.

Statistical Analysis

All calculations were done with GraphPad Prism (GraphPad Software, La Jolla, California). Findings of analyses of images from a perfusion experiment were averaged and used as individual data points. These data were normally distributed and compared using the 2-tailed paired Student *t* test. For the VWF dose response, linear regression was used. Data from the mesenteric perfusion model and the inflammatory endocarditis model were analyzed with the Mann–Whitney *U* test to compare ranks. To compare survival, we used the log-rank test. All values are

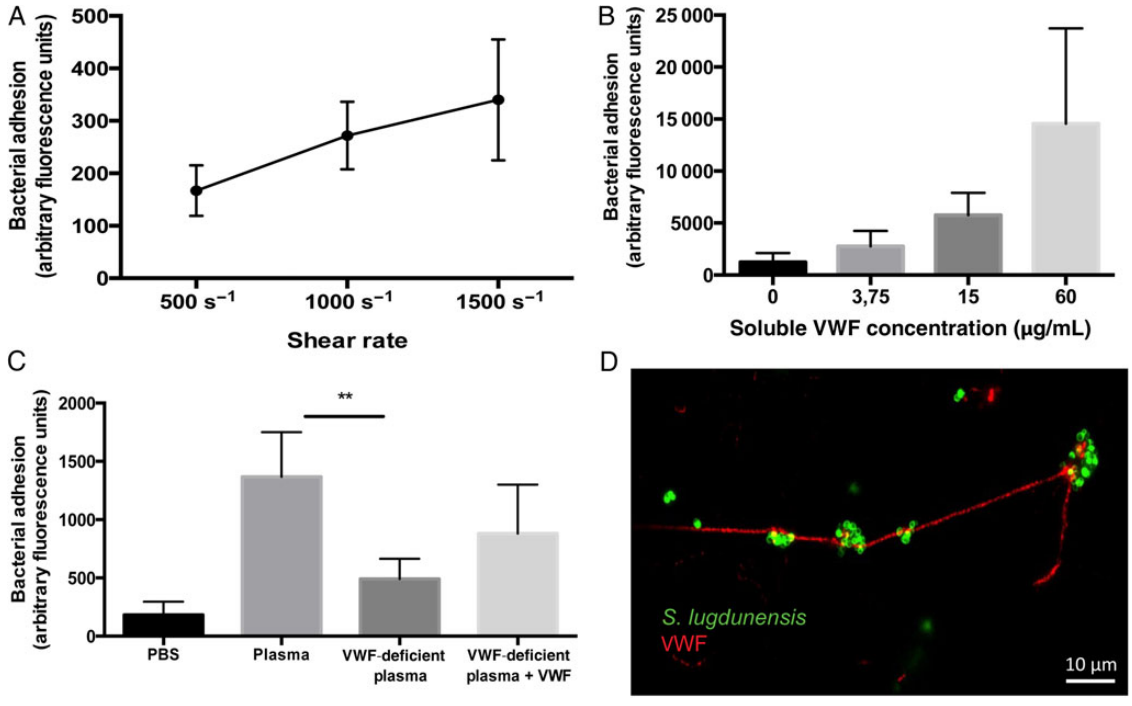

Figure 2. *Staphylococcus lugdunensis* binds to von Willebrand factor (VWF) under flow conditions. *A*, Micro-parallel flow chamber perfusion of fluorescent-labeled *S. lugdunensis* N920143 over VWF-coated (50 µg/mL) coverslips at shear rates ranging from 500 s^{-1} to 1500 s^{-1} (n = 7). *B*, Perfusion of collagen-coated coverslips with fluorescent-labeled *S. lugdunensis* N920143 at a shear rate of 1000 s^{-1} in the presence of soluble VWF at different concentrations as indicated (n = 8; slope = 106.6 ± 21.19; *P* = .001, by linear regression). *C*, Perfusion of *S. lugdunensis* N920143 over collagen-coated coverslips in the presence of phosphate-buffered saline (PBS), human plasma, VWF-deficient plasma, or VWF-deficient plasma supplemented with VWF (60 µg/mL; n = 4). All results are expressed as mean ± SD. $^{**}P < .01$, by the 2-tailed paired Student *t* test. *D*, Immunofluorescent image (original magnification ×630) of collagen-coated coverslips after perfusion with fluorescent-labeled *S. lugdunensis* N920143 (green) in human plasma with immunostaining for VWF (red).

reported as mean ± standard deviation (SD) or median ± interquartile range if appropriate. A P value of <.05 was considered statistically significant.

RESULTS

S. lugdunensis Binds Directly to VWF Under Flow Without the Need for Platelets

Using light transmission aggregometry, we investigated whether *S. lugdunensis* induces platelet activation. In contrast to *S. aureus*, *S. lugdunensis* did not activate platelets when added to PRP, even at very high concentrations (10^8 CFU/mL; Figure 1*A*). Moreover, platelets did not influence bacterial adhesion under flow. We evaluated this by perfusing fluorescent-labeled *S. lugdunensis* in a parallel flow chamber and measuring bacterial adhesion to collagen in the presence of buffer, human plasma, or PRP. In plasma, *S. lugdunensis* bound approximately 4-fold more efficiently to collagen as compared to buffer (n = 6; P = .011). Adding platelets, however, did not enhance bacterial adherence (Figure 1*B*).

We hypothesized that *S. lugdunensis* binds directly to VWF and evaluated the interaction with VWF under flow by perfusing fluorescent-labeled *S. lugdunensis* over VWF-coated surfaces. *S. lugdunensis* bound to VWF at shear rates ranging from 500 s^{-1} to 1500 s^{-1}, and binding to VWF persisted with increasing shear rates (Figure 2*A*).

To quantify the adhesion of *S. lugdunensis* to the subendothelium, we did perfusion experiments over collagen-coated surfaces. When perfusions were performed in PBS, *S. lugdunensis* bound poorly to collagen. However, when soluble VWF was added, the adhesion to collagen increased in a concentration-dependent manner (n = 8; slope = 106.6 ± 21.2; P = .001; Figure 2*B*).

These experiments were repeated with normal and VWF-deficient human plasma. With normal plasma, the adhesion of *S. lugdunensis* to collagen increased significantly, compared with experiments done in buffer. However, when VWF-deficient plasma was used, adhesion to collagen was reduced (n = 4; P < .01). Conversely, when VWF-deficient plasma was reconstituted with VWF, the adhesion of *S. lugdunensis* tended to increase (Figure 2*C*). Immunofluorescence staining of a collagen-coated coverslip that had been perfused with *S. lugdunensis* in the presence of plasma confirmed the bacterial binding to VWF (Figure 2*D*).

S. lugdunensis Has a Unique Mechanism for Binding to VWF That Involves the A2 Domain and an Unidentified Bacterial Ligand

S. aureus and *S. lugdunensis* are unique among staphylococci in their ability to bind VWF under flow. Figure 3*A* shows the binding of several staphylococcal species to collagen in the presence or absence of VWF. Adding VWF improved the adhesion of *S. aureus* and *S. lugdunensis* but not that of other staphylococci.

To explore which domains of VWF are responsible for interacting with *S. lugdunensis*, we performed flow experiments over collagen-coated surfaces, adding either soluble WT VWF or VWF deletion mutants that lack specific regions in the molecule. The A3 deletion mutant did not increase binding efficacy,

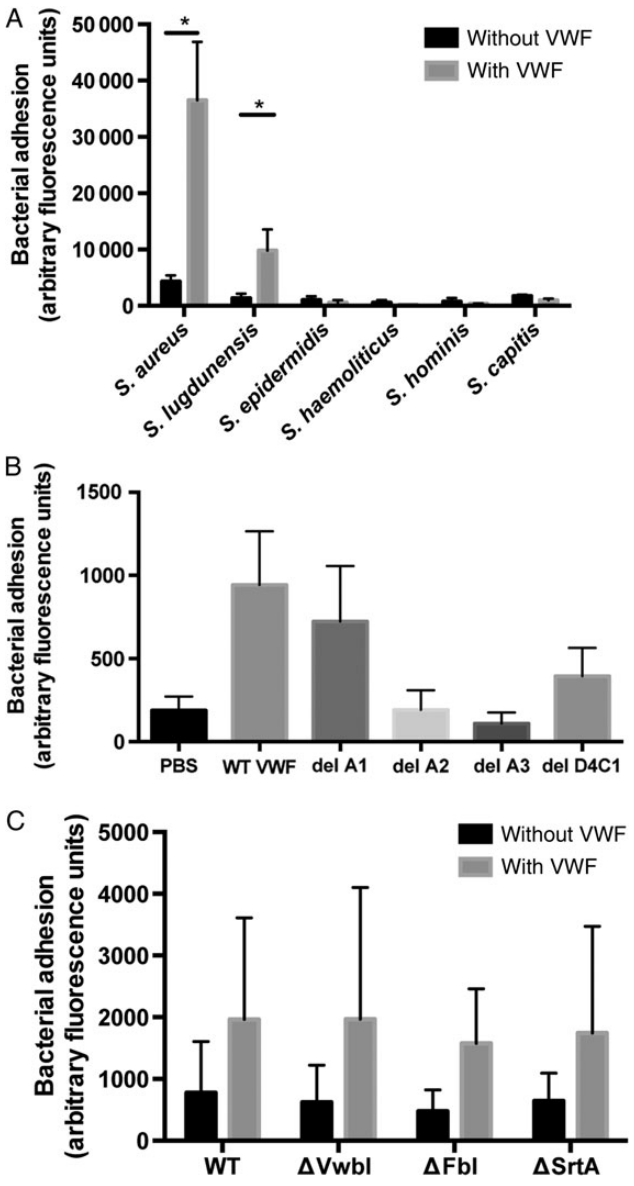

Figure 3. *Staphylococcus lugdunensis* has a unique mechanism for binding to von Willebrand factor (VWF) that involves the A2 and A3 domains and does not occur via the VWF-binding protein (vWbl). *A–C*, Micro-parallel flow chamber perfusion (shear rate, 1000 s^{-1}) over collagen-coated glass coverslips (0.16 mg/mL) with fluorescent-labeled bacteria. All results are expressed as mean ± SD. *P < .05, by the 2-tailed paired Student t test. *A*, Adhesion of various staphylococcal species to collagen in the absence or presence of soluble VWF (60 µg/mL; n = 5). *B*, Perfusion with *S. lugdunensis* N92143 over collagen in the presence of soluble wild-type (WT) VWF or VWF deletion mutants that lack the A1, A2, A3, or D4C1 domains. *C*, Binding to collagen of WT *S. lugdunensis* N920143 or *S. lugdunensis* mutants that lack the vWbl, fibrinogen-binding protein, or sortase A gene (ΔvWbl, ΔFbl, and ΔSrtA, respectively) in the presence or absence of VWF (n = 7). Abbreviations: *S. aureus, Staphylococcus aureus; S. epidermidis, Staphylococcus epidermidis; S. haemolyticus, Staphylococcus haemolyticus; S. hominis, Staphylococcus hominis; S. capitis, Staphylococcus capitis.*

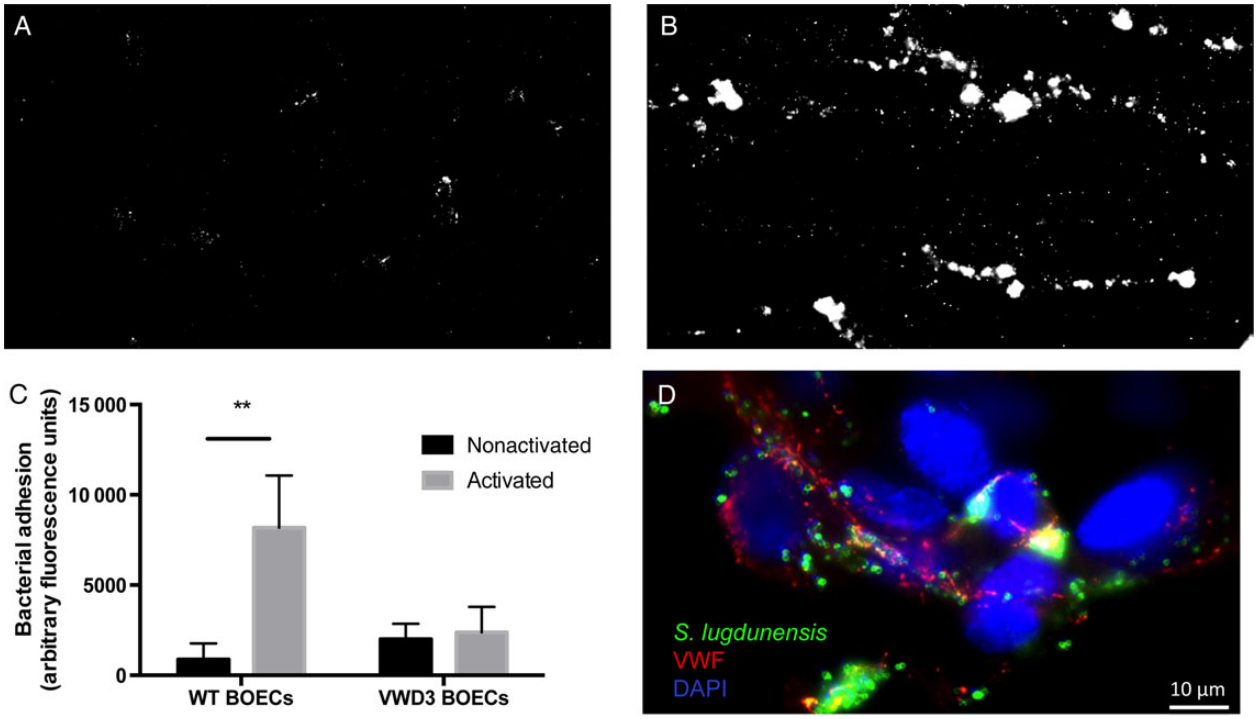

Figure 4. Binding of *Staphylococcus lugdunensis* to activated endothelial cells is mediated by von Willebrand factor (VWF). Micro-parallel flow chamber perfusions of human blood outgrown endothelial cells (BOECs) with fluorescent-labeled *S. lugdunensis* N920143 at a shear rate of 1000 s^{-1}. Where indicated, the cells were first activated by perfusion with the Ca^{2+}- ionophore A23187 (0.1 mM) to trigger VWF release. *A* and *B*, Representative example (original magnification ×200) of *S. lugdunensis* adhering to resting endothelial cells (*A*) and to activated endothelium (*B*). *C*, Binding of *S. lugdunensis* to resting or activated BOECs isolated from healthy volunteers (wild-type [WT]WT BOECs) and to BOECs from a patient with type 3 von Willebrand disease (VWD3 BOECs). Results are expressed as mean ± SD (n ≥ 3). $^{**}P < .01$, by the 2-tailed paired Student *t* test. *D*, Fluorescence image (original magnification ×630) of *S. lugdunensis* (green) adhering to activated endothelium under flow with immunostaining for VWF (red) and DAPI staining of the cell nucleus (blue).

in line with the requirement of the A3 domain for collagen binding. Increased binding to collagen was, however, observed after adding the A1 or D4C1 deletion mutants to the perfusate. Interestingly, no increased collagen adhesion was observed after addition of the A2 deletion mutant (Figure 3*B*).

The bacterial receptor of *S. lugdunensis* for VWF has been postulated to be the vWbl [10]. However, *S. lugdunensis* mutants that lacked vWbl bound as efficiently to VWF as did WT bacteria. Similarly, mutants with deficiencies in the genes encoding Fbl and SrtA were still able to interact with VWF (Figure 3*C*). Additionally, we found that bacteria in the stationary growth phase adhered better to VWF than those in the exponential phase (Supplementary Figure 1*A*). The ability to bind VWF was confirmed for 4 clinical strains of patients with *S. lugdunensis* bacteremia (Supplementary Figure 2*B*).

Adhesion of *S. lugdunensis* to Activated Endothelial Cells Is Dependent on VWF

To investigate whether VWF is important for the adhesion of *S. lugdunensis* to endothelial cells, we mounted our flow chamber with a confluent layer of BOECs and perfused the cells with fluorescent-labeled bacteria at a shear rate of 1000 s^{-1}.

Figure 4*A* illustrates the poor binding of *S. lugdunensis* to resting endothelium. In contrast, when BOECs were first activated with the calcium ionophore A23187 to trigger VWF release, bacterial adhesion increased >5-fold (n = 5; $P < .01$; Figure 4*B* and 4*C*).

Conversely, when perfusions were done over BOECs isolated from a patient who lacks functional VWF (resulting in type 3 von Willebrand disease), *S. lugdunensis* adhesion remained poor, even after endothelial cell activation (n = 3) (Figure 4*C*). The binding of *S. lugdunensis* to VWF multimers secreted from activated endothelial cells was confirmed by immunofluorescence staining (Figure 4*D*).

VWF Mediates the Adhesion *of S. lugdunensis* to the Vessel Wall In Vivo

Next, we studied the interaction between *S. lugdunensis* and the vasculature in a mesenteric perfusion model [8]. We visualized the intestinal microvasculature of C57Bl/6 mice with an inverted microscope and injected fluorescent-labeled bacteria to observe the interaction of *S. lugdunensis* with the vessel wall in real time (Figure 5*A* and 5*B*).

Similar to our observations in endothelial cells, *S. lugdunensis* adhered poorly to resting endothelium. In contrast, when the vasculature was activated by local application of

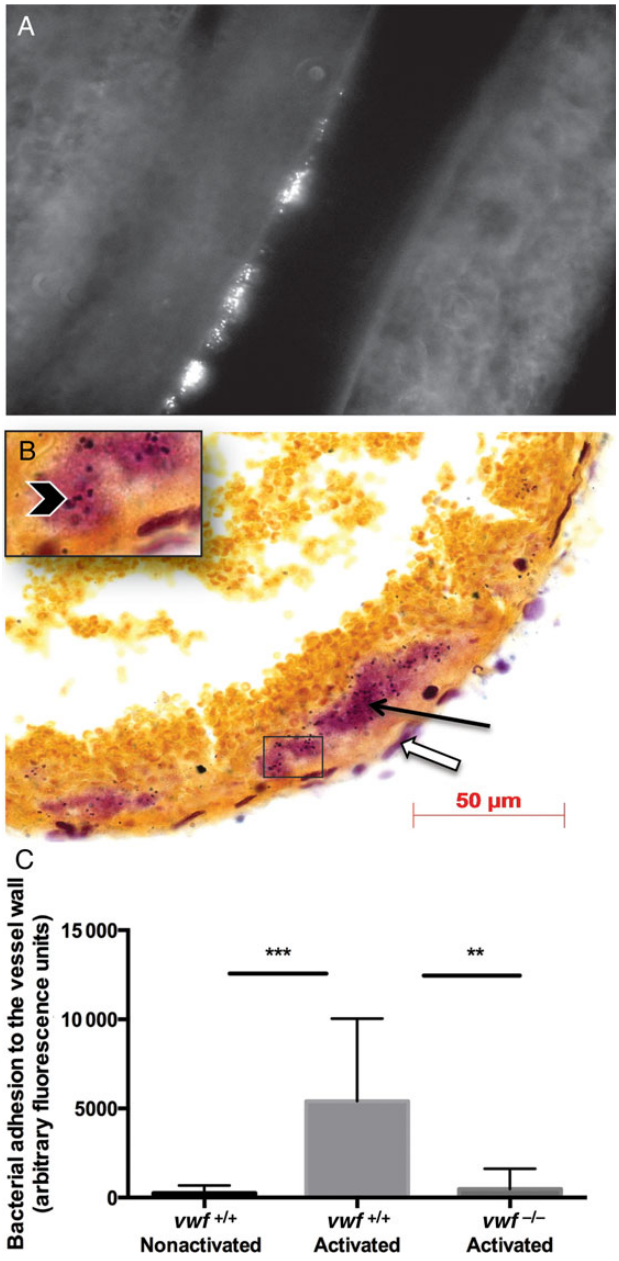

Figure 5. Adhesion of *Staphylococcus lugdunensis* to activated vascular endothelium in vivo is mediated by von Willebrand factor (VWF). *A–C*, In vivo venous mesenteric perfusion model in which the abdomen of C57Bl/6 mice was opened and the mesenteric microcirculation was visualized with an inverted microscope. To trigger VWF release, the vascular endothelium was activated by local application of 5 µL of the Ca^{2+}-ionophore A23187 (10 mM). Subsequently, fluorescent-labeled *S. lugdunensis* N920143 (3×10^7 colony-forming units) was injected via a jugular vein catheter, and binding to vessel wall was assessed by measuring the fluorescence signal. *A*, Representative image of fluorescent-labeled *S. lugdunensis* adhering to the activated vessel wall. *B*, Gram staining of a mesenteric vein (original magnification ×1000) after local activation and subsequent injection of *S. lugdunensis*, showing a lesion (black arrow) with individual staphylococci (arrowhead) adhering to the vascular endothelium (white arrow). *C*, Binding of *S. lugdunensis* to the vessel wall in wild-type mice (*vwf* $^{+/+}$), with or without activation of the vascular endothelium, compared with binding of *S. lugdunensis* in VWF knockout mice (*vwf* $^{-/-}$) after activation. Results are expressed as median + interquartile range (n = 39). $^{**}P < .01$ and $^{***}P < .001$, by the Mann–Whitney test, to compare ranks.

the calcium ionophore A23187, bacteria started rolling on the vessel wall and were able to adhere (Video S1). In consequence, bacterial adhesion increased 16-fold after endothelial cell activation (n = 24; $P < .001$; Figure 5*B*). However, in VWF knockout (*vwf* $^{-/-}$) mice, the adhesion of *S. lugdunensis* to the vasculature was reduced compared to WT mice (n = 31; $P < .002$; Figure 5*C*).

A New Model of Inflammation-Induced Endocarditis Corroborates the Importance of VWF in *S. lugdunensis* Valve Infection

Next, we investigated whether VWF plays a role in the development of *S. lugdunensis* endocarditis by using a standard mouse model of endocarditis. In this model, a wire was advanced beyond the aortic valve to generate valve damage, and bacteria were injected intravenously 24 hours after surgery. In this model, we found no difference in mortality between WT and *vwf* $^{-/-}$ mice (n = 18; $P = .48$; Figure 6*A*). However, histologic analysis of the infected aortic valves revealed that the lesions were mainly located in a fibrin clot that surrounded the inserted wire (Figure 6*B*).

Henceforth, this model mimics foreign body infections, rather than native valve endocarditis. We therefore have developed a model that more accurately simulates the initial pathogenesis of endocarditis. Since endocarditis often develops on inflamed, rather than damaged, heart valves, we tested whether endocarditis could be generated by inflammation. To this end, we introduced a small catheter into the carotid artery and advanced it beyond the aortic valve. Subsequently, histamine was infused to locally activate the valve endothelium. This was followed by a 10-minute perfusion with *S. lugdunensis* (3×10^5 CFUs).

To assess the initial adhesion of *S. lugdunensis*, we euthanized the mice immediately after infusion and harvested the hearts for histologic analysis. Figure 7*A* and 7*B* shows the adhesion of *S. lugdunensis* to the aortic valve leaflets after activation of the valve endothelium. We quantified bacterial adhesion by measuring the intensity in fluorescence after infusing fluorescent-labeled bacteria. If no histamine was used, hardly any bacteria adhered to the valves. In contrast, endothelial cell activation with histamine recruited large amounts of *S. lugdunensis* to the valve leaflets (n = 16; $P < .001$; Figure 7*C*), but this was less pronounced in *vwf* $^{-/-}$ mice (n = 21; $P < .05$; Figure 7*C*). These results were confirmed by measuring vegetation size by Gram staining (Supplementary Figure 2*A*) and by CFU count on lysates of the hearts (Supplementary Figure 2*B*).

In an additional set of experiments, we performed histologic analysis of aortic valves from mice 3 days after the procedure. As illustrated in Figure 7*D*, Gram staining of an aortic valve showed large bacterial vegetations in mice that survived the surgical procedure, confirming that local inflammation triggers bacterial retention and induces endocarditis. Survival analysis (Supplementary Figure 2*C*) showed no mortality in mice that did not receive

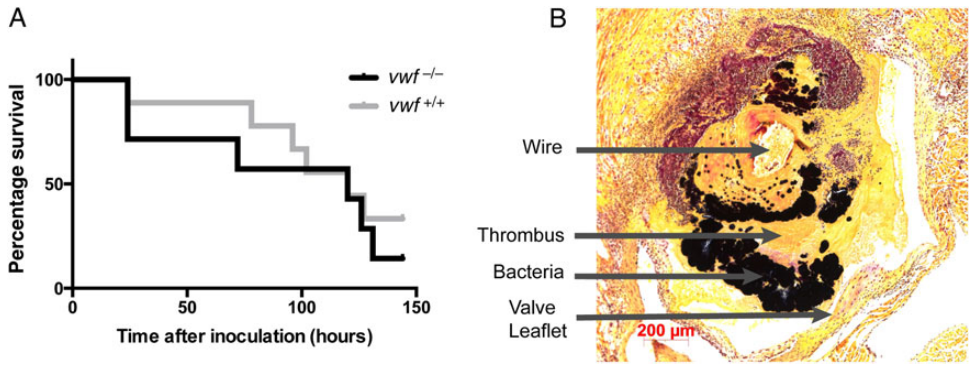

Figure 6. Von Willebrand factor (VWF) does not play a significant role in a standard wire mouse model of *Staphylococcus lugdunensis* endocarditis. A small wire was inserted in the carotid artery of C57Bl/6 mice and advanced beyond the aortic valve. To induce valve damage, the wire was left in place and *S. lugdunensis* N920143 (3×10^6 colony-forming units) was injected intravenously via tail vein 24 hours after surgery. *A*, Survival proportion of wild type mice ($vwf^{+/+}$) and VWF knockout mice ($vwf^{-/-}$; n = 18). *P* = .48, by the log-rank test, to compare survival. *B*, Representative image (original magnification ×100) of a Gram stain of the aortic valve at day 3 after surgery.

histamine. By day 7, 30% of mice in which histamine was infused had died, with a trend toward improved survival in $vwf^{-/-}$ mice.

DISCUSSION

We showed that *S. lugdunensis* binds directly to VWF, allowing shear-resistant adhesion to the subendothelial matrix and to the inflamed vascular endothelium. Unlike most other endocarditis pathogens, *S. lugdunensis* is incapable of binding and activating platelets. The direct binding of VWF may therefore be one of the key initial steps in the development of *S. lugdunensis* endocarditis. The significance of these findings is further strengthened by our observation that VWF binding is a unique feature of *S. aureus* and *S. lugdunensis*. Indeed, other coagulase-negative staphylococci are unable to interact with VWF under flow. Shear-resistant binding to VWF may therefore explain why *S. lugdunensis* causes more-aggressive infections, such as endocarditis, compared with other coagulase-negative staphylococci.

The initial adhesion of bacteria to the cardiac valves is a prerequisite for further vegetation formation [15]. *S. aureus* has a redundancy of surface adhesins that enable it to bind to endothelial cells or to subendothelial matrix proteins. These adhesins are either proteins that are covalently bound to the cell wall (microbial surface components recognizing adhesive matrix molecules [MSCRAMMs]) [16] or ligands that are secreted but can bind back to the bacterial surface (secretable expanded repertoire adhesive molecules [SERAMs]) [17]. MSCRAMMs such as clumping factor A and the fibronectin-binding proteins have been well characterized, and their role in infective endocarditis is established [18, 19]. However, when bacteria are faced with considerable shear forces, the binding efficiency of these adhesins will decrease [20]. The VWF-binding protein of *S. aureus* is an exception to this rule. The binding of this SERAM to VWF is actually shear dependent, meaning that when shear stress increases, binding efficiency also increases [8].

In contrast to the extended knowledge on the *S. aureus* adhesins, little is known about their counterparts in *S. lugdunensis*. Like *S. aureus, S. lugdunensis* has a SrtA gene that covalently anchors MSCRAMMs with an LPXTG motive to the cell wall [21]. Sequencing of the *S. lugdunensis* N920143 genome has revealed 11 genes encoding LPXTG proteins [22]. Among them are vWbl and Fbl, the only 2 MSCRAMMs that have been studied. Fbl is a protein that shares high similarity with *S. aureus* clumping factor A [23]. VWbl on the other hand has no structural resemblance to any of the *S. aureus* MSCRAMMs and has been put forward as a potential ligand for VWF [10]. However, to date, it has not been shown that vWbl promotes adhesion to VWF, and neither the deletion of vWbl nor of Fbl affected the outcome of endocarditis in a rat model [11].

In our experiments, a vWbl deletion mutant showed the same binding to VWF as the WT strain. It might be that vWbl does not represent a functional VWF-binding protein. Alternatively, the protein might not be expressed under the conditions used in our experiments. However, our data show that the adherence to VWF is mediated by a factor that remains unknown.

Interestingly, *SrtA* mutants were also able to bind VWF. This suggests that VWF binding may involve a secreted protein, similar to the VWF-binding protein of *S. aureus* and not a cell-wall-anchored protein. Nonetheless, there are no genes in the *S. lugdunensis* genome that bear homology with the VWF-binding protein of *S. aureus*. Moreover, we found clear differences in the mechanisms between *S. aureus* and *S. lugdunensis* VWF binding. *S. aureus* binds to the A1 domain of VWF [8], but based upon flow experiments with VWF deletion mutants, we believe that, for *S. lugdunensis*, the A2 and not the A1 domain is involved.

Nonetheless, in both *S. aureus* and *S. lugdunensis,* VWF proved to be essential in the adhesion to the vascular endothelium and subendothelial matrix under shear stress. Considering *S. lugdunensis*' propensity to cause endocarditis and the fact

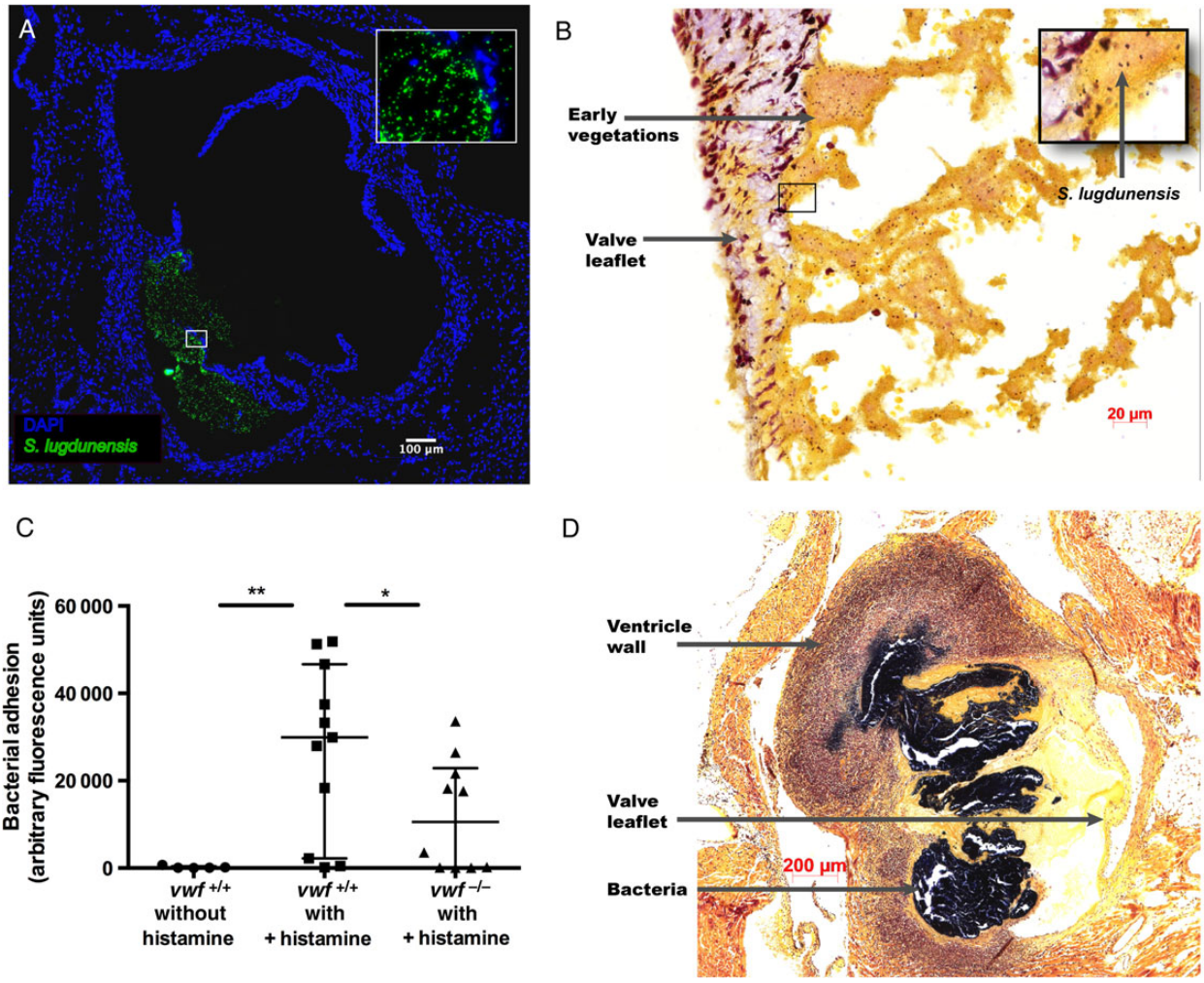

Figure 7. A new model of inflammation induced infective endocarditis corroborates the importance of von Willebrand factor (VWF) in *Staphylococcus lugdunensis* endocarditis. A small polyethylene catheter was inserted in the carotid artery and advanced beyond the aortic valve of C57Bl/6 mice. The valvular endothelium was locally activated through infusion of histamine (200 mM at an infusion rate of 10 µL/min) for 5 minutes, followed by infusion of *S. lugdunensis* (3×10^6 colony-forming units/mL) for 10 minutes. *A* and *B*, Cross-sections of the aortic valve of mice that were euthanized immediately after the procedure. *A*, Fluorescence image (original magnification ×100) of fluorescent-labeled *S. lugdunensis* (green) adhering to the aortic valve, stained with DAPI (blue) after subtraction of autofluorescent elastin fibers. *B*, Gram staining (original magnification ×1000) of a lesion on an aortic valve leaflet. *C*, Adhesion of fluorescent-labeled *S. lugdunensis* to the valve leaflets immediately after the procedure in wild-type mice ($vwf^{+/+}$) and VWF knockout mice ($vwf^{-/-}$) mice, in the presence or absence of histamine. Results are expressed as median ± interquartile range (n = 21). *$P < .05$ and **$P < .01$. *D*, Gram staining of the aortic valve at day 3 of a mouse that survived the procedure.

that heart valves are subjected to considerable shear stress, one can therefore easily speculate on a role for VWF in *S. lugdunensis* endocarditis.

To study this, we first used the standard mouse endocarditis model as described in the literature [14]. This model relies on cardiac valve damage, generated by the insertion of a wire or catheter through the aortic valve. Although this model is used extensively [14, 24, 25], it is not without its flaws. Our histologic analysis showed that, when a wire is inserted trough the aortic valve, a fibrin clot around the wire is formed. Bacteria tend to adhere to this clot, rather than infecting the valve leaflets. Hence, it is not surprising that we were unable to establish a role for VWF in this model, since it relies heavily on fibrin binding. In consequence, this model simulates foreign body infection more than native valve endocarditis.

To overcome these shortcomings, we developed a model that did not require heart valve damage or the presence of foreign material. This is in accordance with the observation that 40% of patients with native valve endocarditis have structurally normal heart valves [26]. The lesions in these patients are thought to originate on inflamed, rather than damaged, heart valves.

We therefore generated a model in which we could elicit infective endocarditis by inducing inflammation. This was done by local infusion of histamine, a potent endothelial cell activator. When we subsequently infused *S. lugdunensis*, we indeed observed bacteria attaching to the heart valves. After docking

to the valves, these bacteria eventually gave rise to large endocarditis vegetations.

These findings support the hypothesis that inflamed heart valves can act as a substrate for bacterial adhesion in infective endocarditis. Our model therefore better represents endocarditis in patients with structurally normal heart valves, compared with older models. Moreover, this model gives us a unique glimpse into the early stage of infective endocarditis. Henceforth, it might serve as a useful tool to further study this disease. Our results already indicate that VWF release represents a crucial step in the early development of *S. lugdunensis* endocarditis.

In summary, we believe that the binding of *S. lugdunensis* to VWF is crucial in infective endocarditis. However, our study has limitations. We did not identify the bacterial ligand for VWF but merely excluded the most known MSCRAMMs. Further research should focus on additional virulence factors of *S. lugdunensis* and on eluding the mechanism of binding to VWF.

Supplementary Data

Supplementary materials are available at http://jid.oxfordjournals.org. Consisting of data provided by the author to benefit the reader, the posted materials are not copyedited and are the sole responsibility of the author, so questions or comments should be addressed to the author.

Notes

Acknowledgments. We thank Prof J. Verhaegen, for collection of clinical strains; Prof K. Peerlinck, for patient samples; and K. Cludts and S. Van kerckhoven, for their skillful technical assistance.

Financial support. This work was supported by the Research Foundation Flanders (FWO; grant 11S5414N; fellowships to L. L., M. P., and C. V.; and support to P. V., a senior clinical investigator at the FWO).

Potential conflicts of interest. All authors: No reported conflicts. All authors have submitted the ICMJE Form for Disclosure of Potential Conflicts of Interest. Conflicts that the editors consider relevant to the content of the manuscript have been disclosed.

References

1. Frank KL, Del Pozo JL, Patel R. From clinical microbiology to infection pathogenesis: how daring to be different works for *Staphylococcus lugdunensis*. Clin Microbiol Rev **2008**; 21:111–33.
2. Anguera I, Del Rio A, Miro JM, et al. *Staphylococcus lugdunensis* infective endocarditis: description of 10 cases and analysis of native valve, prosthetic valve, and pacemaker lead endocarditis clinical profiles. Heart **2005**; 91:e10.
3. Zwaginga JJ, Sakariassen KS, Nash G, et al. Flow-based assays for global assessment of hemostasis. Part 2: current methods and considerations for the future. J Thromb Haemost **2006**; 4:2716–7.
4. Yoganathan AP, He Z, Casey Jones S. Fluid mechanics of heart valves. Annu Rev Biomed Eng **2004**; 6:331–62.
5. Huck V, Schneider MF, Gorzelanny C, Schneider SW. The various states of von Willebrand factor and their function in physiology and pathophysiology. Thromb Haemost **2014**; 111:598–609.
6. Cox D, Kerrigan SW, Watson SP. Platelets and the innate immune system: mechanisms of bacterial-induced platelet activation. J Thromb Haemost **2011**; 9:1097–107.
7. Vanassche T, Kauskot A, Verhaegen J, et al. Fibrin formation by staphylothrombin facilitates *Staphylococcus aureus*-induced platelet aggregation. Thromb Haemost **2012**; 107:1107–21.
8. Claes J, Vanassche T, Peetermans M, et al. Adhesion of *Staphylococcus aureus* to the vessel wall under flow is mediated by von Willebrand factor-binding protein. Blood **2014**; 124:1669–76.
9. Pappelbaum KI, Gorzelanny C, Grassle S, et al. Ultralarge von Willebrand factor fibers mediate luminal *Staphylococcus aureus* adhesion to an intact endothelial cell layer under shear stress. Circulation **2013**; 128:50–9.
10. Nilsson M, Bjerketorp J, Wiebensjo A, Ljungh A, Frykberg L, Guss B. A von Willebrand factor-binding protein from *Staphylococcus lugdunensis*. FEMS Microbiol Lett **2004**; 234:155–61.
11. Heilbronner S, Hanses F, Monk IR, Speziale P, Foster TJ. Sortase A promotes virulence in experimental *Staphylococcus lugdunensis* endocarditis. Microbiology **2013**; 159:2141–52.
12. Lankhof H, Damas C, Schiphorst ME, et al. von Willebrand factor without the A2 domain is resistant to proteolysis. Thromb Haemost **1997**; 77:1008–13.
13. Ingram DA, Mead LE, Tanaka H, et al. Identification of a novel hierarchy of endothelial progenitor cells using human peripheral and umbilical cord blood. Blood **2004**; 104:2752–60.
14. Gibson GW, Kreuser SC, Riley JM, et al. Development of a mouse model of induced *Staphylococcus aureus* infective endocarditis. Comp Med **2007**; 57:563–9.
15. Werdan K, Dietz S, Loffler B, et al. Mechanisms of infective endocarditis: pathogen-host interaction and risk states. Nat Rev Cardiol **2014**; 11:35–50.
16. Foster TJ, Hook M. Surface protein adhesins of *Staphylococcus aureus*. Trends Microbiol **1998**; 6:484–8.
17. Chavakis T, Wiechmann K, Preissner KT, Herrmann M. *Staphylococcus aureus* interactions with the endothelium: the role of bacterial "secretable expanded repertoire adhesive molecules" (SERAM) in disturbing host defense systems. Thromb Haemost **2005**; 94:278–85.
18. Heying R, van de Gevel J, Que YA, Moreillon P, Beekhuizen H. Fibronectin-binding proteins and clumping factor A in *Staphylococcus aureus* experimental endocarditis: FnBPA is sufficient to activate human endothelial cells. Thromb Haemost **2007**; 97:617–26.
19. Que YA, Haefliger JA, Piroth L, et al. Fibrinogen and fibronectin binding cooperate for valve infection and invasion in *Staphylococcus aureus* experimental endocarditis. J Exp Med **2005**; 201:1627–35.
20. Reddy K, Ross JM. Shear stress prevents fibronectin binding protein-mediated *Staphylococcus aureus* adhesion to resting endothelial cells. Infect Immun **2001**; 69:3472–5.
21. Mazmanian SK, Liu G, Ton-That H, Schneewind O. *Staphylococcus aureus* sortase, an enzyme that anchors surface proteins to the cell wall. Science **1999**; 285:760–3.
22. Heilbronner S, Holden MT, van Tonder A, et al. Genome sequence of *Staphylococcus lugdunensis* N920143 allows identification of putative colonization and virulence factors. FEMS Microbiol Lett **2011**; 322:60–7.
23. Nilsson M, Bjerketorp J, Guss B, Frykberg L. A fibrinogen-binding protein of *Staphylococcus lugdunensis*. FEMS Microbiol Lett **2004**; 241:87–93.
24. Panizzi P, Nahrendorf M, Figueiredo JL, et al. In vivo detection of *Staphylococcus aureus* endocarditis by targeting pathogen-specific prothrombin activation. Nat Med **2011**; 17:1142–6.
25. Ring J, Hoerr V, Tuchscherr L, Kuhlmann MT, Loffler B, Faber C. MRI visualization of *Staphyloccocus aureus*-induced infective endocarditis in mice. PLoS One **2014**; 9:e107179.
26. Olmos C, Vilacosta I, Fernandez C, et al. Comparison of clinical features of left-sided infective endocarditis involving previously normal versus previously abnormal valves. Am J Cardiol **2014**; 114:278–83.